Transition between Saturation Regimes of Gyrokinetic Turbulence

D. R. Hatch,[1,2,*] F. Jenko,[2,3] A. Bañón Navarro,[2] and V. Bratanov[2]

[1]*Institute for Fusion Studies, University of Texas at Austin, Austin, Texas 78712, USA*
[2]*Max Planck Institute for Plasma Physics, EURATOM Association, 85748 Garching, Germany*
[3]*Max-Planck/Princeton Center for Plasma Physics*

(Received 18 June 2013; published 22 October 2013)

A gyrokinetic model of ion temperature gradient driven turbulence in magnetized plasmas is used to study the injection, nonlinear redistribution, and collisional dissipation of free energy in the saturated turbulent state over a broad range of driving gradients and collision frequencies. The dimensionless parameter L_T/L_C, where L_T is the ion temperature gradient scale length and L_C is the collisional mean free path, is shown to parametrize a transition between a saturation regime dominated by nonlinear transfer of free energy to *small perpendicular* (to the magnetic field) scales and a regime dominated by dissipation at *large* scales in *all* phase space dimensions.

DOI: 10.1103/PhysRevLett.111.175001 PACS numbers: 52.30.Gz, 52.35.Ra, 52.65.Tt

Introduction.—Gyrokinetic theory is the predominant formalism for describing low-frequency microturbulence in magnetized plasmas [1], with a wide range of applications from magnetic confinement fusion [2,3] to space and astrophysics [4–6]. Despite its importance, a coherent overall picture regarding the fundamental nature of gyrokinetic turbulence has yet to emerge. In this context, it is key to understand the injection, nonlinear redistribution, and collisional dissipation of free energy—which is the ideal quadratic invariant in gyrokinetics—in the saturated turbulent state. Because of the diffusive terms (second-order velocity space derivatives) inherent in realistic collision operators, collisional dissipation is often associated with small scales in velocity space. This is roughly analogous to the link between dissipation and small spatial scales in Navier-Stokes turbulence, with the (normalized) collision frequency playing the role of the inverse Reynolds number.

Two main mechanisms have been identified for developing small scales in velocity space: linear phase mixing (Landau damping) [7,8], associated with small scales in parallel (to the magnetic field) velocity space, and nonlinear phase mixing [9,10], which becomes important at $k_\perp \rho_i > 1$ ($k_\perp$ is the perpendicular wave number and ρ_i is the ion gyroradius) and is linked to small scales in perpendicular velocity and real space. In contrast with the latter, a large fraction of the collisional dissipation is often observed to occur at large (real space) perpendicular scales in gyrokinetic simulations [11,12]. This large-scale dissipation has been interpreted using the so-called *damped eigenmode* paradigm [11–13]–saturation via nonlinear excitation of linearly stable structures at phase space scales comparable to those of the driving microinstabilities. To date, there exists no framework reconciling large-scale and small-scale dissipation scenarios. At issue is the relative importance of each of these mechanisms, the processes by which they interact with each other, and the parameters that determine transitions between different saturation regimes.

In this work, we exploit the transparency of a relatively simple gyrokinetic system in order to address these questions. We study electrostatic ion temperature gradient (ITG) driven turbulence in slab geometry using a Hermite representation for the parallel velocity space. The Hermite free energy spectrum, which is steeper than is expected linearly, is interpreted using the concept of *critical balance* [14–16]. These insights are used to reconcile different saturation paradigms. In particular, it is shown that the dimensionless parameter L_T/L_C, where L_T is the ion temperature gradient scale length and L_C is the collisional mean free path, parameterizes a transition from a regime where the bulk of the free energy achieves dissipation via nonlinear transfer to small perpendicular scales (for very small L_T/L_C) to a regime where the dissipation is dominated by dynamics on large scales in *all* phase space dimensions (for larger L_T/L_C). The transition is observed to occur in the weakly collisional regime at a critical value of L_T/L_C on the order of 10^{-3}.

Gyrokinetic model.—We study the nonlinear gyrokinetic equations in unsheared slab geometry, using the adiabatic electron approximation. The real space dimensions are subjected to a Fourier representation, while the parallel velocity space is decomposed in terms of Hermite polynomials, $f(v) = \sum_{n=0}^{\infty} \hat{f}_n H_n(v) e^{-v^2}$, where $H_n(x) \equiv (n! 2^n \pi^{1/2})^{-1/2} e^{x^2} (-d/dx)^n e^{-x^2}$. Hermite polynomials provide an elegant characterization of energy transfer and dissipation in parallel velocity scales [17,18]. Moreover, they have recently been shown to optimally represent velocity space in gyrokinetic simulations [19] and to facilitate accurate solutions of linear kinetic operators [20]. The resulting gyrokinetic equation reads [21]

$$\frac{\partial \hat{f}_{\mathbf{k},n}}{\partial t} = \frac{\eta_i i k_y}{\pi^{1/4}} \frac{k_\perp^2}{2} \bar{\phi}_{\mathbf{k}} \delta_{n,0} - \frac{i k_y}{\pi^{1/4}} \bar{\phi}_{\mathbf{k}} \delta_{n,0} - \frac{\eta_i i k_y}{2^{1/2} \pi^{1/4}} \bar{\phi}_{\mathbf{k}} \delta_{n,2} - \frac{i k_z}{\pi^{1/4}} \bar{\phi}_{\mathbf{k}} \delta_{n,1} - i k_z (\sqrt{n} \hat{f}_{\mathbf{k},n-1} + \sqrt{n+1} \hat{f}_{\mathbf{k},n+1}) - \nu n \hat{f}_{\mathbf{k},n} + \sum_{\mathbf{k}'} (k'_x k_y - k_x k'_y) \bar{\phi}_{\mathbf{k}'} \hat{f}_{\mathbf{k}-\mathbf{k}',n}, \quad (1)$$

where $\hat{f}_{\mathbf{k},n}(\rho_i n_{i0}/L_n v_{ti}^3)$ is the ion distribution function, n_{i0} is the ion density, L_n is the density gradient scale length, v_{ti} is the ion thermal velocity, n denotes the order of the Hermite polynomial, $t(L_n/v_{ti})$ is time, $\eta_i = L_n/L_T$ is the ratio of the gradient scale lengths, $k_y(\rho_i^{-1})$ is the Fourier wave number for the direction perpendicular to both the direction of the background gradients [$x \rightarrow k_x(\rho_i^{-1})$] and the coordinate aligned with the magnetic field [$z \rightarrow k_z(L_n^{-1})$]. The perpendicular wave number is $k_\perp \equiv (k_x^2 + k_y^2)^{1/2}$, $\bar{\phi}_{\mathbf{k}}(\rho_i T_{e0}/L_n e)$ is the gyro-averaged electrostatic potential, T_{e0} is the background electron temperature, e is the elementary charge, and $\nu(v_{ti}/L_n)$ is the collision frequency. We use the Lenard-Bernstein collision operator [22] for the parallel velocity, for which Hermite polynomials are eigenvectors: $\nu \partial_v[(1/2)\partial_v + v] \rightarrow \nu n$. Equation (1) has been integrated over perpendicular velocity, replacing the gyroaverage operators with factors of $e^{-k_\perp^2/2}$—an exact result if the perturbed distribution function is a Maxwellian in $v_\perp$. The electrostatic potential is determined by the field equation

$$\phi_{\mathbf{k}} = \pi^{1/4} e^{-k_\perp^2/2} \hat{f}_{\mathbf{k},0} / [\tau + 1 - \Gamma_0(k_\perp^2)], \quad (2)$$

where τ is the ratio of the ion to electron temperature, and $\Gamma_0(x) \equiv e^{-x} I_0(x)$, with I_0 the zeroth order modified Bessel function. Note that here we do not remove the flux-surface-averaged potential, as this treatment strongly suppresses the turbulence in slab simulations [17]. This $v_\perp$-integrated gyrokinetic system is well justified for $k_\perp < 1$ [23]. In the numerical results described below, simulations are limited to these scales. By doing this, we intentionally neglect nonlinear phase mixing (which becomes important at $k_\perp > 1$), and model dissipative processes at $k_\perp > 1$ using hyperdiffusion.

Free energy balance.—The $\mathbf{k}$- and n-resolved evolution equation for the free energy $\varepsilon_{\mathbf{k},n} = \varepsilon_{\mathbf{k}}^{(\phi)} \delta_{n,0} + \varepsilon_{\mathbf{k},n}^{(f)}$ with the electrostatic part $\varepsilon_{\mathbf{k}}^{(\phi)} \equiv \frac{1}{2}[\tau + 1 - \Gamma_0(k_\perp^2)]^{-1} |\phi_{\mathbf{k}}|^2$ and the entropy part $\varepsilon_{\mathbf{k},n}^{(f)} \equiv \frac{1}{2} \pi^{1/2} |\hat{f}_{\mathbf{k},n}|^2$ is readily derived with the help of Eqs. (1) and (2). One thus obtains

$$\frac{\partial \varepsilon_{\mathbf{k},n}^{(f)}}{\partial t} = \eta_i Q_{\mathbf{k}} \delta_{n,2} - C_{\mathbf{k},n} - J_{\mathbf{k}}^{(\phi)} \delta_{n,1} + J_{\mathbf{k},n-1/2} - J_{\mathbf{k},n+1/2} + N_{\mathbf{k},n}^{(f)}, \quad (3)$$

where the energy injection rate $\eta_i Q_{\mathbf{k}} = \eta_i \Re[-(\pi^{1/4}/2^{1/2}) i k_y \hat{f}_{\mathbf{k},2}^* \bar{\phi}]$ is proportional to the radial ion heat flux $Q_{\mathbf{k}}$ and limited to $n = 2$, the collisional dissipation rate is $C_{\mathbf{k},n} = 2\nu n \varepsilon_{\mathbf{k},n}^{(f)}$, $J_{\mathbf{k}}^{(\phi)}$ is the energy transferred between the electrostatic component at $n = 0$ and the entropy component (i.e., Landau damping), $J_{\mathbf{k},n-1/2} \equiv \Re[-\pi^{1/2} i k_z \sqrt{n} \hat{f}_{\mathbf{k},n}^* \hat{f}_{\mathbf{k},n-1}]$ ($J_{\mathbf{k},n+1/2} \equiv \Re[\pi^{1/2} i k_z \sqrt{n+1} \hat{f}_{\mathbf{k},n}^* \hat{f}_{\mathbf{k},n+1}]$), defines energy transfer between $n-1$ ($n+1$) and n (i.e., phase mixing), and $N_{\mathbf{k},n}^{(f)}$ is the contribution from the nonlinearity. The latter redistributes energy in k space in a conservative manner. Similarly, the phase mixing terms represent conservative energy transfer in n space, as reflected in the $J_{\mathbf{k},n\pm1/2}$ notation. Thus, the $\mathbf{k}$- and n-summed energy equation reduces to a balance of the net energy sources $\eta_i Q$ and sinks C. The scales (in the the full phase space) at which this balance is achieved depend on the interplay between the dissipation and the conservative energy transfer channels, which is the focus of the remainder of this Letter.

Simulations.—A fully spectral code (called DNA) has been developed to solve the system defined by Eqs. (1) and (2). The simulations use a (normalized) box size of 125.7 (increased to 144.4 in some simulations) in the x and y directions, and resolve up to $k_{x,y}^{(\max)} = 1.55$. Hyperdiffusion [15] of the form $\nu_\perp (k_{x,y}/k_{x,y}^{(\max)})^8 \hat{f}_{\mathbf{k},n}$ is employed in the perpendicular spatial directions in order to cut off the spectrum at $k_\perp \sim 1.0$. For the parallel direction, the (normalized) box size is 62.8, and the simulations resolve up to $k_z = 4.7$. In the literature, $k = 0$ modes are often artificially deleted [17,24] for slab ITG simulations. We opt to dynamically evolve all $k = 0$ modes and implement a Krook damping term for $k_z = 0$ and $k_z = k_z^{(\min)}$ modes in order to avoid slowly growing low-k_z modes that fail to saturate (this is only necessary at very low collisionality and/or high gradient drive). This Krook term is always a small fraction of the total dissipation. In combination with the collision operator, we use hypercollisions [25] of the form $\nu_h (n/n_{\max})^8 \hat{f}_{\mathbf{k},n}$ in order to cut off the Hermite spectra more sharply in the dissipation range. $n_{\max}$ and ν_h are selected in combination with $k_z^{(\max)}$ to satisfy two criteria: (i) dissipation due to the hypercollisions becomes important only for $n > n_c$, where n_c characterizes the scale at which collisionality begins to dominate the phase mixing cascade, and (ii) $\nu_h > k_z^{(\max)} \sqrt{n_{\max}+1}$. The latter criterion, when used in conjunction with the boundary condition [25] $\hat{f}_{n_{\max}+1} = i k_z \sqrt{n_{\max}+1} \hat{f}_n / (\nu_h)(n_{\max} + 1/n_{\max})^8$ is sufficient to ensure that the tails of the Hermite spectra are completely smooth at the $n_{\max}$ boundary.

Critical balance and Hermite spectra.—First, we would like to characterize the Hermite free energy spectra. The steady-state $n \gg 1$ version of the energy evolution equation, Eq. (3), can be approximated as $|k_z|(\partial/\partial n)\sqrt{n} \varepsilon_{\mathbf{k},n} = N_{\mathbf{k},n}^{(f)} - 2\nu n \varepsilon_{\mathbf{k},n}$ [17,18]. By summing over k space, this becomes $(\partial/\partial n)\langle k_z \rangle_n \sqrt{n} \varepsilon_n = -2\nu n \varepsilon_n$, where $\varepsilon_n \equiv \sum_{\mathbf{k}} \varepsilon_{\mathbf{k},n}$, and the characteristic parallel wave number for the nth-order Hermite polynomial is

$$\langle k_z \rangle_n \equiv \frac{\sum_{\mathbf{k}} |k_z| \varepsilon^{(f)}_{\mathbf{k},n}}{\sum_{\mathbf{k}} \varepsilon^{(f)}_{\mathbf{k},n}}. \quad (4)$$

In cases with fixed k_z, this equation can produce spectra with $n^{-1/2}$ power laws [18,25]. In the model used in this work, the characteristic parallel scale length is free to adjust to the turbulent dynamics, and the n dependence of $\langle k_z \rangle_n$ is necessary for determining the Hermite spectrum. We postulate, and numerically verify, that the nonlinear decorrelation rate ω_n^{NL} determines this n-dependent parallel scale length via the relation $\omega_n^{NL} \sim \langle k_z v_{ti} \rangle_n$. This is, in effect, a type of *critical balance* [14–16] applied to moments of all orders.

We first test the concept of critical balance in the limiting case $\nu \to 0$, which we approximate by setting $\nu = 0$, keeping only hyper-collisions and resolving up to $n_{\max} = 256$. The correlation function $R_{k_\perp,n}(\tau) = \int \hat{f}^*_{k_\perp,n}(t+\tau)\hat{f}_{k_\perp,n}(t)dt / \int |\hat{f}_{k_\perp,n}|^2 dt$, where $\hat{f}_{k_\perp,n} \equiv \sum_{k_z} \hat{f}_{\mathbf{k},n}$, is shown in Fig. 1 along with the characteristic parallel streaming time $\langle k_z v_{ti} \rangle_n^{-1}$ for three representative values of $k_\perp$. The close connection between $\langle k_z v_{ti} \rangle_n^{-1}$ and contours of $R_{k_\perp,n}$ demonstrates critical balance. Note that the result is the same if the correlation function is calculated for the actual nonlinear term in Eq. (1) instead of $\hat{f}_{k_\perp,n}$.

The observed $\sqrt{n}$ dependence of the nonlinear decorrelation rate is inconsistent with the naive scaling argument $\omega_n^{NL} \sim \mathcal{N}_{\mathbf{k},n}/\hat{f}_{\mathbf{k},n} \sim k_\perp^2 \bar{\phi}$, which has no n dependence. A plausible explanation for the observed n dependence can be arrived at by noting that, for each n, the electrostatic potential beats with the distribution function, additively combining their characteristic frequencies $\omega^{NL}_{n,\mathbf{k}} \sim \omega_\phi|_{\mathbf{k}'} + \omega_{f_n}|_{\mathbf{k}-\mathbf{k}'}$. If the characteristic frequency for the distribution function is determined by the phase mixing time scale $\omega_{f_n}|_{\mathbf{k}} \sim k_z\sqrt{n}$, then the observed $\sqrt{n}$ dependence is captured for $n \gg 1$.

The $\sqrt{n}$ dependence of the global ($k_\perp$ summed) $\langle k_z \rangle_n$ is clearly observed for the three driving gradients examined ($\eta_i = [5.0, 7.5, 10.0]$), and can be explicitly incorporated into the $n \gg 1$ energy equation,

$$\frac{\partial}{\partial n} n\varepsilon_n = -\frac{2\nu}{k_z^{(\mathrm{eff})}} n\varepsilon_n - S_n, \quad (5)$$

where $k_z^{(\mathrm{eff})} \equiv \langle k_z \rangle_n / \sqrt{n}$. In this equation, an energy sink term S_n has been added which could represent, e.g., dissipation due to nonlinear phase mixing. In our simulations, S_n represents high-$k_\perp$ hyperdiffusion, or if one considers the limited range $k_\perp < 1$, nonlinear energy transfer to higher $k_\perp$. If we assume a simple relation $S_n = \alpha\varepsilon_n$, then Eq. (5) has solutions of the form

$$\varepsilon_n = c_0 n^{-1-\alpha} e^{-2\nu n / k_z^{(\mathrm{eff})}}; \quad (6)$$

i.e., due to the extra factor of $\sqrt{n}$, the energy equation supports power laws with *arbitrary* exponents, depending on the rate of energy extraction due to S_n. For the artificial scenario $S_n = 0$, Eq. (5) produces n^{-1} power laws—verified numerically and shown in Fig. 2(a). Note that a spectral exponent of -1 is a critical exponent separating collisional dissipation spectra that increase with n from those that decrease with n. When $\alpha > 0$ (i.e., whenever S_n is an energy sink), the Hermite spectrum is steeper than n^{-1}, and the collisional dissipation peaks at large scales in parallel velocity space. A hypothetical analogous scenario for Navier-Stokes turbulence would be observed if power spectra were steeper than k^{-2}: the scales of energy dissipation would be reversed. Consistent with Eq. (6), various power laws are observed in our simulations depending on the value of $\nu_\perp$. The spectra shown in Fig. 2(b) exhibit a

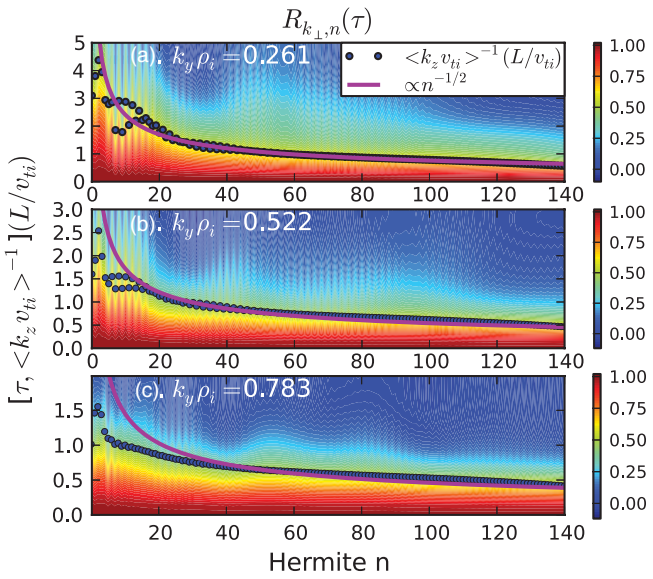

FIG. 1 (color). Contour plots of the temporal correlation function $R_{k_\perp,n}(\tau)$ for three representative wave numbers, $k_x = 0$, $k_y\rho_i = 0.26$ (a), $k_x = 0$, $k_y\rho_i = 0.52$ (b), $k_x = 0$, $k_y\rho_i = 0.78$ (c). Note that the characteristic parallel streaming time $\langle k_z v_{ti} \rangle_n^{-1}$ (dots) tracks the contours of $R_{k_\perp,n}(\tau)$.

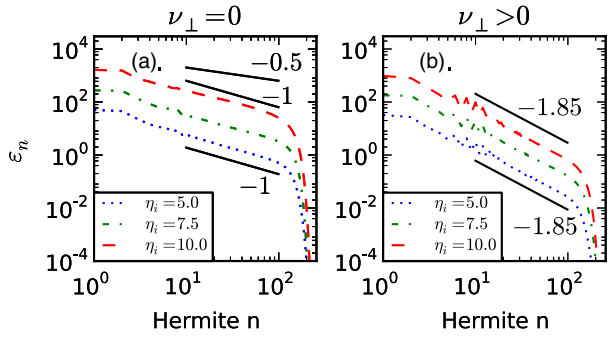

FIG. 2 (color online). Hermite spectra of the free energy $\varepsilon_n^{(f)}$ for three different values of the normalized temperature gradient η_i. The spectra are consistent with the power laws defined in Eq. (6) for cases with $\nu_\perp = 0$ (a) and $\nu_\perp \neq 0$ (b).

$n^{-1.85}$ power law, which is achieved independently for the three driving gradients by increasing $\nu_\perp$ until the appropriate [15] perpendicular energy spectrum $\varepsilon_{k_{x,y}} \propto k_{x,y}^{-7/3}$ is observed between the outer scale and $k_\perp \sim 1$.

Two saturation regimes.—Having characterized the Hermite spectra, we now apply this knowledge to the saturation paradigms outlined in the introduction. As a result of the strongly decreasing (with n) dissipation spectra, large scales in velocity space can make a significant contribution to the dissipation. Since the velocity space structures of the linear eigenmodes that drive the turbulence are strongly peaked at low n, it is not surprising that collisional dissipation peaks at the same perpendicular scales as the energy drive. This is the case for the model studied here [as seen in Fig. 3(a)], as well as for, to the best of our knowledge, all other published gyrokinetic dissipation spectra (see, e.g., Refs. [11,12,17,26–28]). This is consistent with the damped eigenmode paradigm; nonlinear energy transfer from the unstable modes will primarily produce structures with comparable scales in velocity space since the nonlinearity does not (directly) couple different n. This will be explored in detail in a future publication.

This analysis also suggests regimes where this low-$k_\perp$ dissipation scenario will no longer hold. The collision frequency determines how much energy is dissipated at each n [compare Figs. 3(b) and 3(d)], and by extension, how much energy remains to be transferred nonlinearly to $k_\perp \gtrsim 1$ where the much faster nonlinear perpendicular phase mixing cascade takes over. Likewise, the normalized driving gradient η_i determines the amplitude of ϕ, and by extension the rate of nonlinear energy transfer to $k_\perp > 1$. Thus, it may be expected that a dimensionless parameter incorporating both of these quantities $L_T/L_C = \eta_i^{-1}\nu$ determines a transition between two saturation regimes.

An estimate of these two processes can be made by exactly expressing the collisional dissipation as $C_{k_\perp \lesssim 1} = \nu \sum_{k_\perp \lesssim 1} \sum_{k_z} \sum_n n\varepsilon^{(f)}_{\mathbf{k},n}$, and approximating the nonlinear energy flux [28] as $\Pi_{k_\perp \sim 1} \sim \sum_{k_z} \sum_n \omega^{NL}_{k_\perp \sim 1} \varepsilon^{(f)}_{k_z,n,k_\perp \sim 1}$ ($k_\perp \sim 1$ denotes a sum over a shell of wave numbers with magnitude $k_\perp \sim 1$). The normalized nonlinear decorrelation rate at $k_\perp \sim 1$ is expected to be somewhat smaller than η_i, and is observed in our simulations to obey $\omega^{NL}_{k_\perp \sim 1} \sim \beta_{k_\perp \sim 1}\eta_i$, with $\beta_{k_\perp \sim 1} \lesssim 0.3$ (taking for simplicity the n-summed quantity). The relative importance of the two mechanisms can thus be estimated as $C_{k_\perp \lesssim 1}/\Pi_{k_\perp \sim 1} \sim \epsilon_d^{-1} L_T/L_C$, where

$$\epsilon_d^{-1} \equiv \frac{\sum_{k_\perp \lesssim 1} \sum_{k_z} \sum_n n\varepsilon^{(f)}_{\mathbf{k},n}}{\sum_{k_z} \sum_n \beta_{k_\perp \sim 1} \varepsilon^{(f)}_{k_z,n,k_\perp \sim 1}}. \quad (7)$$

Note that both the numerator and the denominator in Eq. (7) entail sums over the free energy, but the contribution from the collisional dissipation (numerator) is larger because it is a *global* sum in $k_\perp$, and the prefactor increases more strongly with n. This suggests that low-$k_\perp$ dissipation can be important even for $L_T/L_C \ll 1$.

We conducted a scan of L_T/L_C for three different ion temperature gradients and for collision frequencies spanning over two orders of magnitude, adjusted to hold L_T/L_C constant at each point in the scan. The ratio of the collisional dissipation C to the dissipation due to $k_\perp$ hyperdiffusion $D_\perp$, is plotted in Fig. 4 (note that the hypercollisions are grouped with the collisions, and the low-k_z dissipation term is not included); the dissipation is dominated by high-$k_\perp$ hyperdiffusion [see Fig. 3(c)] at very low collisionality, and by collisional dissipation at low $k_\perp$ [see Fig. 3(a)] as the collisionality increases. The two dissipation mechanisms are equal at $L_T/L_C \sim 2.7 \times 10^{-3}$, indicating that the low-$k_\perp$ mechanism is important even in weakly collisional regimes (i.e., for $\nu L/v_{ti} \ll 1$). These results are consistent with full toroidal gyrokinetic simulations—e.g., in Ref. [28] the ratio of dissipation at $k_\perp < 1$ to dissipation at $k_\perp > 1$ (similar to the quantity $C/D_\perp$) is found to be approximately one for $L_T/L_C = 1.7 \times 10^{-3}$ [inferred from Fig. (1)b in Ref. [28]]. A modified collision operator (removing collisions at $n = 1$ and $n = 2$ in order to conserve momentum and energy) was also tested and

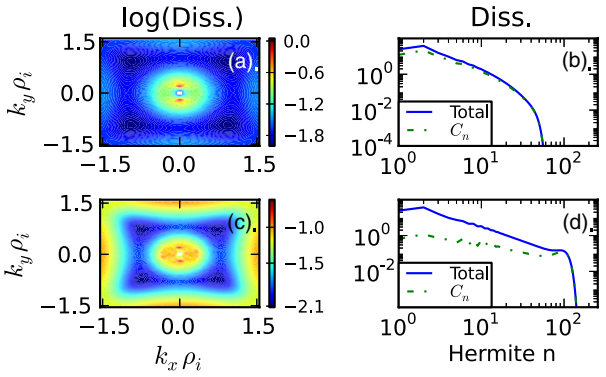

FIG. 3 (color online). Free energy dissipation for two collision frequencies, $L_T/L_C = 6.3 \times 10^{-3}$ (top row), and $L_T/L_C = 2.0 \times 10^{-4}$ (bottom row). Contour plots for the perpendicular wave numbers are shown in (a) and (c), and Hermite spectra are shown in (b) and (d).

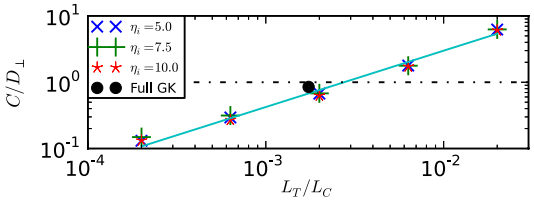

FIG. 4 (color online). The ratio of collisional dissipation C to dissipation from $k_\perp$ hyperdiffusion $D_\perp$ for a scan in L_T/L_C. The black circle denotes a similar quantity (ratio of dissipation at $k_\perp < 1$ to dissipation at $k_\perp > 1$) for the toroidal gyrokinetic simulation described in Ref. [28].

found to decrease the collisional dissipation and increase the low-k_z dissipation. The critical L_T/L_C was shifted to $\sim 6 \times 10^{-3}$, but the major conclusions are unchanged.

Summary.—A fully spectral gyrokinetic model of ion temperature gradient driven turbulence in magnetized plasmas was used to investigate free energy dynamics in quasistationary states. We have shown that even for small values of L_T/L_C the dissipation mainly takes place at large scales in *all* phase space dimensions. As L_T/L_C decreases, collisional dissipation in parallel velocity space at $k_\perp < 1$ is insufficient to balance the free energy injection, and nonlinear perpendicular phase mixing is inferred to be an important dissipation mechanism. This work reconciles two disparate dissipation paradigms for gyrokinetic turbulence.

Useful conversations with M. Barnes, B. Teaca, P. W. Terry, A. Zocco, N. Loureiro, G. Plunk, and S. M. Mahajan are gratefully acknowledged. Simulations were performed at the Texas Advanced Computing Center (TACC) at The University of Texas at Austin. The research leading to these results has received funding from the European Research Council under the European Union's Seventh Framework Programme (FP7/2007-2013)/ERC Grant Agreement No. 277870.

*drhatch@austin.utexas.edu

[1] J. Krommes, Annu. Rev. Fluid Mech. **44**, 175 (2012).
[2] E. J. Doyle *et al.*, Nucl. Fusion **47**, S18 (2007).
[3] X. Garbet, Y. Idomura, L. Villard, and T. H. Watanabe, Nucl. Fusion **50**, 043002 (2010).
[4] G. G. Howes, S. C. Cowley, W. Dorland, G. W. Hammett, E. Quataert, and A. A. Schekochihin, Astrophys. J. **651**, 590 (2006).
[5] G. G. Howes, J. M. TenBarge, W. Dorland, E. Quataert, A. A. Schekochihin, R. Numata, and T. Tatsuno, Phys. Rev. Lett. **107**, 035004 (2011).
[6] M. J. Pueschel, F. Jenko, D. Told, and J. Büchner, Phys. Plasmas **18**, 112102 (2011).
[7] G. W. Hammett, W. Dorland, and F. W. Perkins, Phys. Fluids B **4**, 2052 (1992).
[8] T.-H. Watanabe and H. Sugama, Nucl. Fusion **46**, 24 (2006).
[9] T. Tatsuno, W. Dorland, A. Schekochihin, G. Plunk, M. Barnes, S. Cowley, and G. Howes, Phys. Rev. Lett. **103**, 015003 (2009).
[10] G. Plunk, S. C. Cowley, A. Schekochihin, and T. Tatsuno, J. Fluid Mech. **664**, 407 (2010).
[11] D. R. Hatch, P. W. Terry, F. Jenko, F. Merz, and W. M. Nevins, Phys. Rev. Lett. **106**, 115003 (2011).
[12] D. R. Hatch, P. W. Terry, F. Jenko, F. Merz, M. J. Pueschel, W. M. Nevins, and E. Wang, Phys. Plasmas **18**, 055706 (2011).
[13] P. W. Terry, D. A. Baver, and S. Gupta, Phys. Plasmas **13**, 022307 (2006).
[14] P. Goldreich and S. Sridhar, Astrophys. J. **438**, 763 (1995).
[15] M. Barnes, F. I. Parra, and A. A. Schekochihin, Phys. Rev. Lett. **107**, 115003 (2011).
[16] J. M. TenBarge and G. G. Howes, Phys. Plasmas **19**, 055901 (2012).
[17] T.-H. Watanabe and H. Sugama, Phys. Plasmas **11**, 1476 (2004).
[18] A. Zocco and A. A. Schekochihin, Phys. Plasmas **18**, 102309 (2011).
[19] D. R. Hatch, D. del-Castillo-Negrete, and P. W. Terry, J. Comput. Phys. **231**, 4234 (2012).
[20] V. Bratanov, F. Jenko, D. R. Hatch, and S. Brunner, Phys. Plasmas **20**, 022108 (2013).
[21] The model is similar to that of Ref. [17], except that our model is three dimensional in space and expressed in the Hermite representation.
[22] A. Lenard and I. B. Bernstein, Phys. Rev. **112**, 1456 (1958).
[23] W. Dorland and G. W. Hammett, Phys. Fluids B **5**, 812 (1993).
[24] S. E. Parker, W. Dorland, R. A. Santoro, M. A. Beer, Q. P. Liu, W. W. Lee, and G. W. Hammett, Phys. Plasmas **1**, 1461 (1994).
[25] N. F. Loureiro, A. A. Schekochihin, and A. Zocco, Phys. Rev. Lett. **111**, 025002 (2013).
[26] A. Bañón Navarro, P. Morel, M. Albrecht-Marc, D. Carati, F. Merz, T. Görler, and F. Jenko, Phys. Rev. Lett. **106**, 055001 (2011).
[27] A. Bañón Navarro, P. Morel, M. Albrecht-Marc, D. Carati, F. Merz, T. Gorler, and F. Jenko, Phys. Plasmas **18**, 092303 (2011).
[28] B. Teaca, A. Bañón Navarro, F. Jenko, S. Brunner, and L. Villard, Phys. Rev. Lett. **109**, 235003 (2012).